



1 **Influence of covariance of aerosol and meteorology on co-located precipitating and**
2 **non-precipitating clouds over Indo-Gangetic Plains**

3 Nabia Gulistan¹, Khan Alam¹, Yangang Liu²

4 ¹Department of Physics, University of Peshawar, Peshawar, 25120, Pakistan

5 ²Environmental & Climate Science Department, Brookhaven National Laboratory, USA

6 **Correspondence:** Khan Aalam (khanalam@uop.edu.pk)

7

8

ABSTRACT

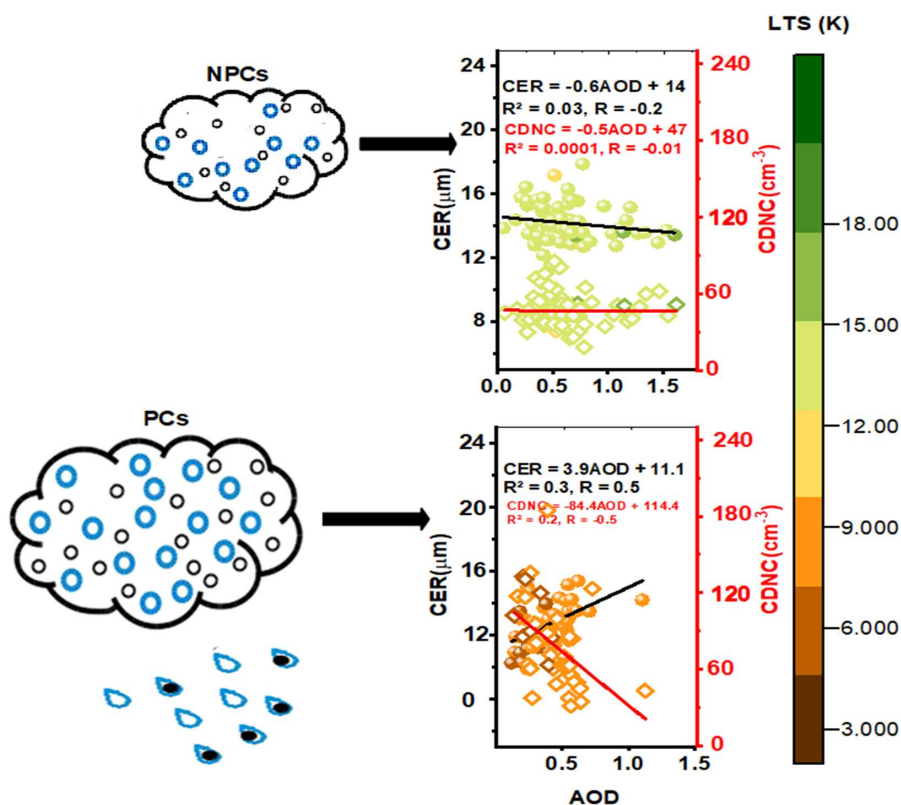
9 Aerosol-cloud-precipitation-interaction (ACPI) plays a pivotal role in the global and regional
10 water cycle and the earth's energy budget; however, it remains highly uncertain due to the
11 underlying different physical mechanisms. Therefore, this study aims to systematically analyze the
12 effects of aerosols and meteorological factors on ACPI in the co-located precipitating (PCs) and
13 non-precipitating clouds (NPCs) clouds in winter and summer seasons by employing the long-term
14 (2001-2021) retrievals from Moderate Resolution Imaging Spectroradiometer (MODIS), Tropical
15 Rainfall Measuring Mission (TRMM), and National Center for Environmental Prediction/National
16 Center for Atmospheric Research (NCEP/NCAR) reanalysis-II datasets over the Indo-Gangetic
17 Plains (IGP). The results exhibit a decadal increase in aerosol optical depth (AOD) over Lahore
18 (5.2%), Delhi (9%), Kanpur (10.7%) and Gandhi College (22.7%) and decrease over Karachi (-
19 1.9%) and Jaipur (-0.5%). The most stable meteorology with high values of lower tropospheric
20 stability (LTS) is found in both seasons over Karachi. In summer season the occurrence frequency
21 of clouds is high (74%) over Gandhi College, 60% of which are PCs. Conversely, the least number
22 of PCs are found over Karachi. Similarly, in winter season, the frequency of cloud occurrence is
23 low over Karachi and high over Lahore and Gandhi College. The analysis of cloud top pressure
24 (CTP) and cloud optical thickness (COT) indicate high values of cloud fraction (CF) for thick and
25 high-level clouds over all study areas except Karachi. The micro-physical properties such as cloud
26 effective radius (CER) and cloud droplet number concentration (CDNC) bears high values (CER
27 $> \sim 15 \mu\text{m}$ and $\text{CDNC} > \sim 50 \text{ cm}^{-3}$) for both NPCs and PCs in summer. The AOD-CER correlation
28 is good (weak) for PCs (NPCs) in winter. Similarly, the sensitivity value of the first indirect effect
29 (FIE) is high (ranged from 0.2 ± 0.13 to 0.3 ± 0.01 in winter, and from 0.19 ± 0.03 to 0.32 ± 0.05
30 in summer) for PCs and low for NPCs. Sensitivity value for second indirect effect (SIE) is



31 relatively high (such as 0.6 ± 0.14 in winters and 0.4 ± 0.04 in summer) than FIE. Sensitivity values
 32 of the aerosol-cloud interaction (ACI) are low (i.e., -0.06 ± 0.09) for PCs in summers. Furthermore,
 33 the precipitation rate (PR) exhibits high values in summer season, and PR values are found high
 34 in comparatively thin clouds with fewer CDNC ($< \sim 50 \text{ cm}^{-3}$) and intermediate for optically thick
 35 clouds with higher CDNC ($> \sim 50 \text{ cm}^{-3}$).

36 **Keywords:** Aerosol-cloud-precipitation-interaction, Aerosol optical depth, cloud effective radius,
 37 cloud droplet number concentration, lower tropospheric stability, relative humidity, first indirect
 38 effect, second indirect effect, precipitation sensitivity.

GRAPHICAL ABSTRACT





53 1. Introduction

54 The aerosol-cloud-precipitation-interaction (ACPI) and aerosol-radiation-interaction (ARI)
55 significantly influence climates at the regional and global scales. Assessing the direct and indirect
56 effects of aerosols is crucial to understand and predict energy budget and the water cycle. In the
57 direct effect, the absorption and scattering of solar radiation by aerosols lead to the warming of the
58 atmosphere and cooling of the earth's surface (Zhou et al., 2020), causing changes in the lower
59 tropospheric stability (LTS) that further leads to modulation of precipitating (PCs) and non-
60 precipitation clouds (NPCs) (Andreae & Rosenfeld, 2008). In the indirect effect, the water-soluble
61 aerosols such as soil dust, sulfates, nitrates, and other organic aerosols ejected naturally and
62 anthropogenically serve as cloud condensation nuclei (CCN) and affect the aerosol-cloud-
63 interaction (ACI) by influencing the growth of cloud droplet and cloud droplet number
64 concentration (CDNC) (Twomey et al., 1977; Albrecht, 1989; Jiang et al., 2002; Chen et al., 2011;
65 Tao et al., 2012). The increase of CDNC and decrease of cloud droplet effective radius (CER)
66 inhibit the onset of precipitation and increase the cloud lifetime (Albrecht, 1989). Conversely, the
67 decrease in CDNC and increase in CER increases the probability of precipitation rate (PR).

68 In the last few decades, most of the cultivable land of the Indo-Gangetic Plain (IGP) has been
69 replaced by urban developments. Due to the fastest growth of population, urbanization,
70 industrialization, and massive combustion of biomass and fossil fuels in residential homes and
71 factories, a decadal increase in aerosols is observed over IGP. The high aerosol loading may affect
72 the formation of tropospheric clouds and seasonal precipitation patterns (Kaskaoutis et al., 2011;
73 Singh et al., 2015; Thomas et al., 2021) and makes IGP suitable for the study of ACPI. Besides,
74 frequent variations in cloud fraction (CF), extreme precipitation and drought abrupt temperature
75 changes (e.g., heat waves), and irregular unseasonal rains may cause major and unavoidable
76 hazards at local and regional levels in the future.

77 In the last two decades, the scientific community has focused on quantification of ACI using both
78 observations (Feingold et al., 2003; Costantino et al., 2010; Zhao et al., 2018, 2020; Anwar et al.,
79 2022) and modeling techniques (Chen et al., 2016, 2018; Wang et al. 2020; Zhou et al., 2020;
80 Sharma et al., 2023). Although, a similar recent study (Anwar et al., 2022) attempted to understand
81 the sensitivities of ACI and the first indirect effect of different subsets of AOD to the different
82 conditions of RH and wind directions and found Twomey effect over the monsoon regions and



83 anti-Twomey effect over the weak and moderately intensive monsoon regions. However, the above
84 study excluded the other significant meteorological parameters such as LTS, PR, and T_{850} and was
85 also limited to the monsoon regions of Pakistan only. Further, in the context of warm rain
86 processes, it is generally understood that the high concentration of aerosols capable of serving as
87 CCN leads to enhanced CDNC known as the FIE or Twomey effect (McCoy et al., 2018). It is also
88 widely acknowledged that CDNC plays a pivotal role in cloud microphysics and significantly
89 influences the onset of precipitation and retention of water in clouds called the second indirect
90 effect (SIE) (Gryspeerd et al., 2016; Naud et al., 2017). Whilst, in the above study, the analysis of
91 CDNC is also not addressed. Therefore, the present study aims to deepen the previous study
92 (Anwar et al., 2022), by a long-term and detailed analysis of the ACPI including aerosol-indirect
93 effects for low-level clouds extended over the whole IGP for understanding different mechanisms
94 of cloud and precipitation formation.

95 This study is focused on estimating the variations in sensitivities of aerosol-cloud relationship to
96 the variations in aerosol loading at specified meteorological conditions for low-level PCs and
97 NPCs in the summer and winter seasons over the IGP. This study is unique in using a large number
98 of samples, classification of clouds in PCs and NPCs, further classification of clouds in low, mid,
99 and high-level clouds through joint COT-CTP histograms, quantification of the sensitivities of FIE,
100 SIE, total indirect effect (TIE), and ACI to CDNC. The significant meteorological parameters
101 considered include temperature at 850 hPa, LTS, relative humidity (RH%) at 850 hPa, vertical
102 velocity (Ω), and PR. Furthermore, by utilizing the Moderate Resolution Imaging
103 Spectroradiometer (MODIS) and Tropical Rainfall Measuring Mission (TRMM) data, the
104 correlation of cloud microphysical properties (CER and CDNC) and AOD at specified values of
105 LTS and cloud liquid water path (CLWP) is examined, and precipitation sensitivity at constant
106 macro-physical condition is estimated.

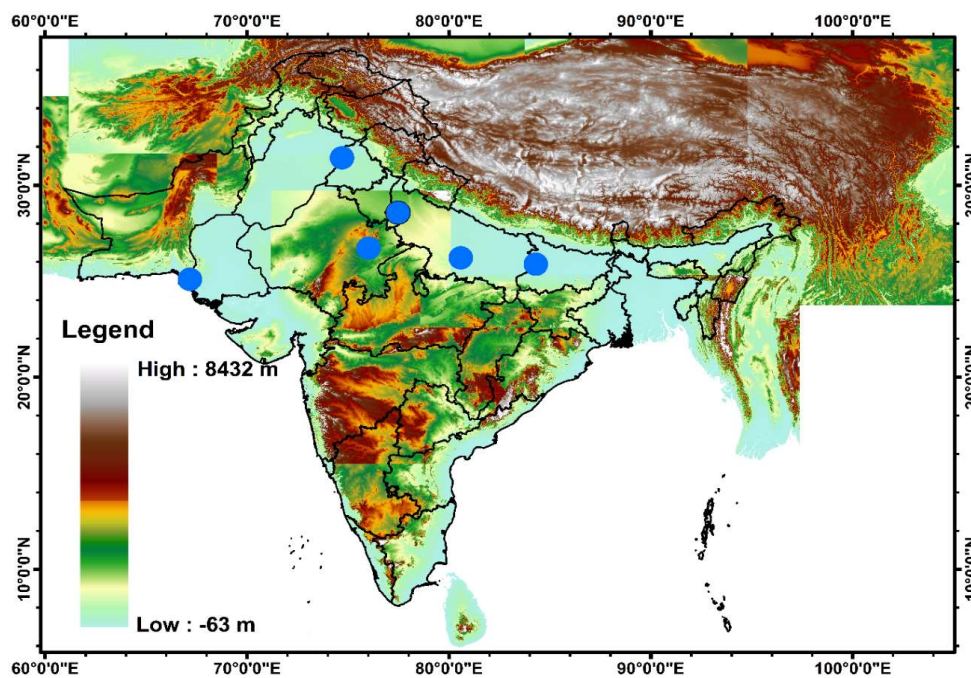
107 **2. Study area and methodology**

108 **2.1. Study area**

109 The selected study area (Fig. 1) comprises the upper and middle portions of the IGP. The upper
110 part consists of the densely populated and developed regions of the eastern part of Pakistan i.e.,
111 Karachi (24.87°N, 67.03°E) and Lahore (31.54°N, 74.32°E) whereas the middle part comprises the



112 northern part of India i.e., Delhi (28.59°N, 77.22°E), Kanpur (26.51°N, 80.23°E), Jaipur (26.91°N,
113 75.81°E) and Gandhi College (25.87°N, 84.13°E).



114
115 Fig. 1. Geographical map of the study area. The blue points show the sites used in this study.

116

117 2.2. Methodology

118 2.2.1. MODIS, NCEP/NCAR reanalysis-II and TRMM data

119 Moderate Resolution Imaging Spectroradiometer (MODIS) is a major constituent of NASA's Earth
120 Observing System (EOS). MODIS is orbiting with two onboard satellites, Terra and Aqua,
121 launched in 1999 and 2002 respectively, with a range of 2330 km spanning the entire globe in a
122 day. It provides data and information with a spatial resolution of x to study atmospheric processes
123 and physical structure (Kedia et al., 2014; Srivastava et al., 2015). This study uses the daily mean
124 of combined dark target and deep blue AOD at 0.55 μm , cloud top pressure (CTP), cloud top
125 temperature (CTT), CF, CER, COT, CDNC, and CLWP from level 3 aerosol-cloud data product
126 MOD08. Data with AOD > 1.5 are excluded to avoid potential misidentification of aerosols as



127 clouds. The following adiabatic approximation (Brenguier et al., 2000; Wood, 2006; Kubar et al.,
128 2009; Michibata et al., 2014) is used to calculate CDNC (cm^{-3}):

$$129 \quad \text{CDNC} = \left(\frac{B}{\text{CER}} \right)^3 * \sqrt{(2 * \text{CLWP} * \gamma_{\text{eff}})}$$

130 (1)

131 Where $B = \sqrt[3]{\left(\frac{3}{4}\pi\rho_{\text{water}}\right)} = 0.0620$, ρ_{water} is the liquid water density, γ_{eff} is the adiabatic
132 gradient of liquid water content in the moist air column (Wood, 2006). Value of γ_{eff} range from 1
133 to 2.5×10^{-3} at a temperature of 32 K to 104 K (Brenguier, 1991; Zhu et al., 2018; Zhou et al.,
134 2020). The CLWP is estimated by use of

$$135 \quad \text{CLWP} = \frac{5\rho_w(\text{CER})(\text{COT})_w}{9},$$

136 (2)

137 Where, ρ_w is the water density at room temperature (Koike et al., 2016).

138 National Center for Environmental Prediction/National Center for Atmospheric Research
139 (NCEP/NCAR) reanalysis datasets provide global reanalysis data sets that combine satellite
140 observations with the simulation of models through data assimilation (Purdy et al., 2016). Daily
141 data for meteorological parameters including temperature, RH%, and Ω at 850 hPa are retrieved
142 at a spatial resolution of T62 Gaussian grid ($1.915^\circ \times 1.875^\circ$) from NCEP reanalysis-II datasets,
143 and used to calculate lower tropospheric stability (LTS) defined as (Li et al., 2017):

$$144 \quad \text{LTS} = \theta_{700} - \theta_0,$$

145 where θ is the potential temperature and the subscripts denote the pressure levels of 700
146 hPa and 1000 hPa.

147 The Tropical Rainfall Measuring Mission (TRMM) is the first Joint satellite mission between
148 NASA America and National Space Development Agency (NASDA) Japan, utilizing the visible
149 infrared and microwaves to measure the rain precipitation over tropical and subtropical regions.
150 The main TRMM instruments that are used to measure rain precipitation are PR and TMI. Where
151 PR is operating at a frequency of 13.8 GHz and TMI is a passive microwave radiometer consisting
152 of nine channels. A calibrated data set TRMM-2B31 of TRMM Combined Instrument (TCI) for



153 TRMM Multi-Satellite Precipitation Analysis (TMPA) is formed from an algorithm that uses TMI
154 and PR. The product TMPA 3B42 gives the rain precipitation averages on a daily and sub-daily
155 basis. In the current study, the data product TMPA or TRMM 3B42 is used for the retrieval of PR
156 on daily basis. The spatial resolution of TRMM 3B42 is $0.25^\circ \times 0.25^\circ$ and is available from the
157 year 1998 to till date.

158 2.2.2. Methodology

159 The present study is designed to analyze and quantify the ACPI for PCs and NPCs in winter and
160 summer under a variety of meteorological conditions. The data are first segregated into two subsets
161 for the summer and winter seasons. Based on precipitation data from TRMM, the subsets are
162 further divided into precipitating and non-precipitating clouds.

163 The sensitivities of cloud parameters to CDNC are analyzed through the following formulation
164 considered from previous studies (Zhou et al., 2020):

$$165 \quad \frac{d\ln(COT)}{d\ln(CDNC)} = -\frac{d\ln(CER)}{d\ln(CDNC)} + \frac{d\ln(CLWP)}{d\ln(CDNC)} \quad (3)$$

167 In this study, the term on the left side of equation (3) is defined as total indirect aerosol effect
168 (TIE), and the first and second terms on the right side of the equation are defined as the first indirect
169 aerosol effect (FIE), and *second indirect effect (SIE)*, respectively. Similarly, the sensitivity
170 of CDNC to AOD is evaluated by employing the index of ACI:

$$171 \quad ACI_{CDNC} = \frac{d\ln(CDNC)}{d\ln(AOD)} \quad (4)$$

173 The sensitivity of PR to CDNC is calculated from the following equation (Jung et al., 2012) :

$$174 \quad S_0 = \left(-\frac{\partial \ln(PR)}{\partial \ln(CDNC)} \right)_{COT} \quad (5)$$



176 **3. Results and Discussion**

177 3.1. Regional and seasonal distribution of AOD

178 AOD is a commonly used proxy for aerosol concentration in the atmosphere and is analyzed here
179 (Fig. 2-3). Fig. 2 shows a meaningful decadal variation in time average maps for combined dark
180 target and deep blue AOD retrieved at $0.55 \mu\text{m}$ over the entire study area for the years (2001-2010)
181 and (2011-2021). Also, Table 1 illustrates the percentage change in decadal averaged values of
182 AOD. The results indicate that AOD exhibits a decrease over Karachi (-1.9%) and Jaipur (-0.5%).
183 Whilst an increase in AOD is observed over Lahore (5.2%), Delhi (9%), Kanpur (10.7%) and
184 Gandhi College (22.7%).

185 Fig.3(a-b) shows the probability density function (PDF) for AOD, illustrating different
186 distributions in summer and winter season. Fig.3a shows that the distribution of AOD over Lahore,
187 Delhi, Kanpur, Jaipur, and Gandhi College is similar. However, a shift in peak value of PDF
188 towards high values of AOD over Lahore and low values over Jaipur illustrate comparatively high
189 and low aerosol concentration in summer season over Lahore and Jaipur respectively. The loading
190 of high concentration of aerosols is owing to the high-density of population, industrialization, and
191 human activities. The major sources of aerosols in all months of the year include vehicular
192 emission originated from old transport facilities, emission of smoke and soot during consumption
193 of biomass for cooking, heavy industrial emission, and aerosols produced in seasonal harvesting
194 and crop-residue burning. All these sources produce organic aerosols which are characterized as
195 hydrophilic particles and have the potential to act as CCN. Likewise, the soil dust particles also
196 act as good CCN due to their hygroscopic nature. Moreover, the meteorological conditions also
197 play a substantial role to enhance AOD values such as the uplifting of loose soil dust and swelling
198 of aerosols due to holding the water vapors (wv) for long time (Masmoudi et al., 2003; Alam et
199 al., 2010, 2011). Also, the lower but flat PDF curve demonstrates low values of AOD over Karachi.

200 As compared to summer season, the pattern of PDF in winter is significantly different as shown in
201 Fig. 3b. The highest peak of PDF for the lowest value of AOD over Karachi illustrates pristine
202 atmosphere. Similarly, the PDF peaks for Lahore, Delhi and Jaipur show comparatively high AOD
203 over Delhi. Likewise, the distribution over Kanpur and Gandhi College is similar illustrating
204 similar values of AOD. The reason for reduced values of AOD in winter season is the wet



205 scavenging and suppressed emission of aerosols from earth surface (Alam et al., 2010; Zeb et al.,
206 2019).

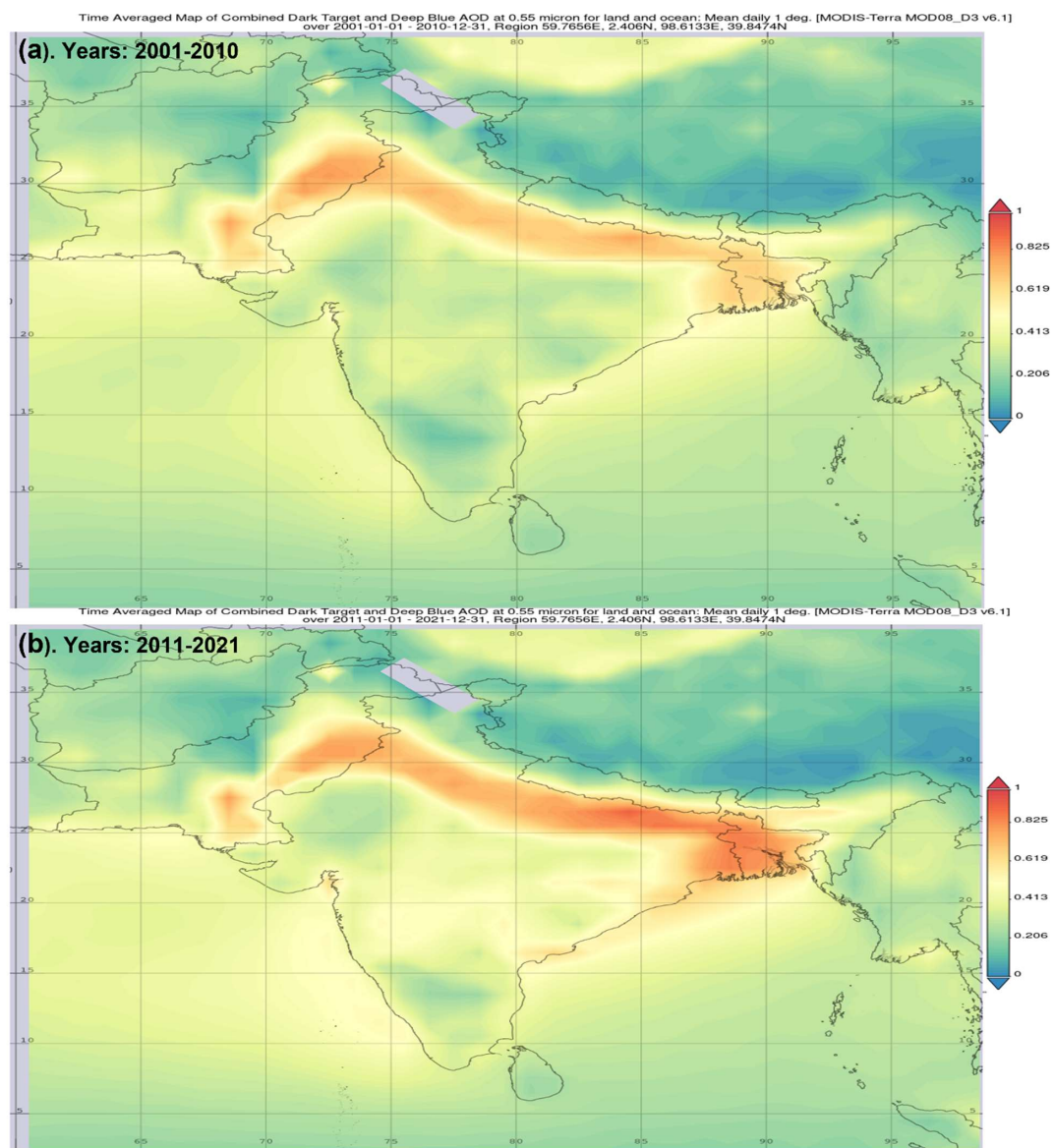
207

208 **Table 1.** Decadal percentage variations in average values of AOD over all study areas.

209

	Karachi	Lahore	Delhi	Kanpur	Jaipur	Gandhi College
Total number of counts	5902	6171	5823	5201	5907	5125
Decadal change in AOD	-1.9%	5.2%	9%	10.7%	-0.5%	22.7%

210



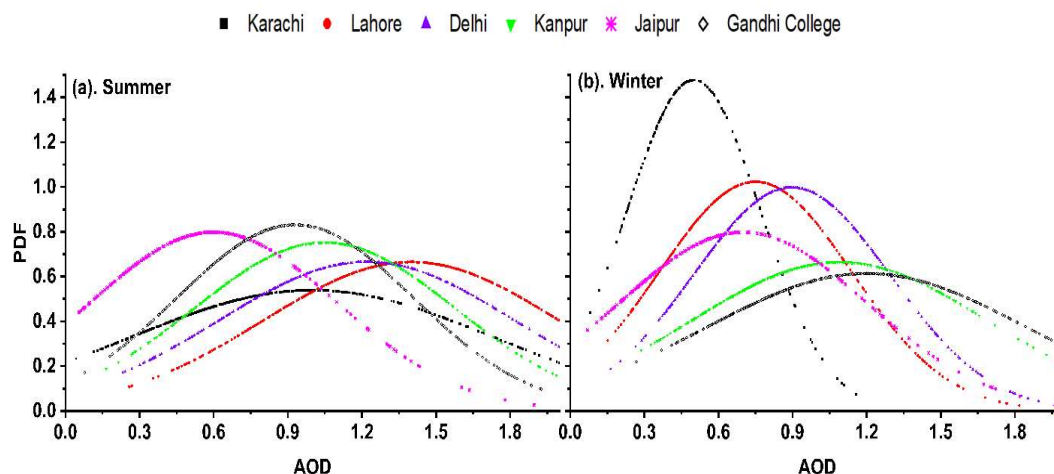
211

212

213

214

Fig. 2. Decadal increase (year: 2001-2010 and 2011-2021) in AOD over study sites.



215

216 **Fig.3.** Probability density function (PDF) of AOD over study sites is shown (a) and (b) for summer and winter seasons
217 respectively.

218 3.2. Climatology of meteorological parameters

219 The variations in meteorological parameters have an unavoidable impact on (estimation of) ACPI.
220 The parameters considered in this study include the temperature, LTS to determine the lower
221 atmospheric stability and the potential for vertical convection that influence the cloud and
222 precipitation formation, the RH% to estimate the level of wv and the Ω to assess the suitable
223 atmospheric dynamics. Fig.4 shows the variations in LTS values for NPCs and PCs in winter and
224 summer season. In winter season, the LTS values are high for NPCs and comparatively lower for
225 PCs over entire study areas. In summer season, the scenario is completely reversed with high
226 values for PCs but low values for NPCs, suggesting stable tropospheric layer on rainy days. This
227 stabilization may be attributed to the cold pools generated by the evaporation of falling rain
228 droplets (Wu et al., 2017). Evidently, the lower LTS values for NPCs in summer season suggests
229 the likelihood of stronger instability that causes high potential of vertical motion and development
230 of thunderstorm. However, Karachi exhibits a distinct pattern of LTS with the highest values in
231 each case, which indicates the existence of the most stable tropospheric layer in Karachi due
232 likely to moist and cold sea breeze due to the city's coastal location.

233 The remaining meteorological parameters considered in this study are listed in Table 2. The high
234 values in each case are indicated in bold and low values are italicized. The results show that in
235 winter season the temperature at 850 hPa (T_{850}) is relatively high for NPCs ranging from 281 ± 2 to

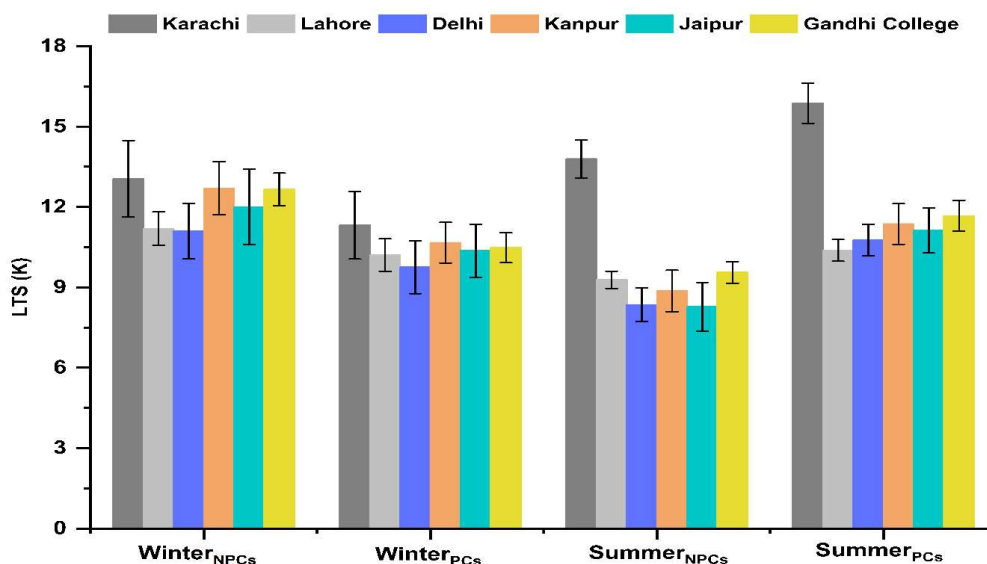


236 286±2 K. The increase in RH% for PCs ranged from 33-57%. Also, the $\Omega > 0$ for NPCs and < 0
 237 for PCs in winter season.

238 In summer season, it is observed that T_{850} is comparatively higher than that for the winter clouds
 239 and ranged from 298±0.4 to 300±0.7 K and 296±0.5 to 298.3±0.6 K for NPCs and PCs
 240 respectively. The high values of T_{850} are due to intense solar fluxes in summer season that keep the
 241 temperature of the earth's surface and adjacent atmospheric layer higher. Also, the increase in
 242 RH% ranged between 25-45 %. The reason for the high values of wv and RH is mainly the suitable
 243 thermodynamical conditions. Besides, during the last two decades, the wv and fog over the Arabian
 244 Sea were increased (Verma et al., 2022). Therefore, the high values of wv and RH in summer
 245 months is due to the high-speed zonal winds that blew in the summer season and transport water
 246 vapors and sea salt from the surface of the Arabian Sea and hydrophilic aerosols such as soil dust
 247 from deserts of Iran, Pakistan, and India to IGP. Where $\Omega < 0$ for PCs over all study areas except
 248 Karachi.

249 The distinct variations in meteorological parameters reveal the occurrence of clouds with diverse
 250 properties. The detailed analysis of such clouds is given in the next subsections.

251



252

253 **Fig. 4.** Variations in lower tropospheric stability (LTS) over all study sites for PCs and NPCs in winter and summer
 254 seasons, the error bars show the standard deviation (SD) values.



Table 2. Meteorological parameters for PCs(NPCs) in summer and winter seasons. Maximum values are for both types of clouds shown in bold and minimum values are indicated as italic.

	Winter Season			Summer Season		
	T ₈₅₀ (K)	RH%	Ω (m/s)	T ₈₅₀ (K)	RH%	Ω (m/s)
Karachi	278±18 (286±2)	70±13.9 (38.3±9)	-0.04±0.04 (0.030.02)	296±0.5 (299±0.84)	68.4±6.7 (45.4±6.2)	0.02±0.04 (-5E-05±0.02)
Lahore	280.5±1 (281±2)	60±5 (36.9±4.4)	-0.04±0.04(0.07±0.02)	298.3±0.6(300±0.7)	63.6±5.2 (35±4.4)	-0.02±0.02 (0.03±0.02)
Delhi	282.5±0.9 (283±0.9)	60.3±9 (35.2±5)	-0.12±0.04(0.04±0.03)	297.4±0.6(299.3±0.8)	64.5±3 (42.5±5.5)	-0.05±0.03 (0.003±0.02)
Kampur	284.3±0.5 (284±0.8)	64.1±4 (37±5)	-0.15±0.03(0.04±0.04)	297±0.6(298.4±0.7)	70.4±5 (46.5±6)	-0.12±0.03 (-0.07±0.03)
Jaipur	284.4±1.3 (284±1)	67.5±6 (40.4±7)	-0.08±0.02(0.04±0.02)	296.7±0.8(299±0.9)	64.9±3 (50.6±4.2)	-0.03±0.02 (-0.03±0.01)
Gandhi College	283.3±0.5 (284.3±0.7)	72±5 (31.6±5)	-0.12±0.05(0.05±0.03)	297±0.4(298±0.4)	71.6±3 (54±4)	-0.16±0.03 (-0.01±0.03)



3.3. Regional and seasonal distribution of clouds and precipitations

3.3.1. Regional and seasonal differences in clouds occurrence and its microphysical structure

Fig.5 shows the frequency of occurrence of precipitable clouds and total number of cloudy days. To avoid any overestimation, the data are filtered to include COT and $CF > 5$. The results show that in the winter season the frequency of clouds is low over Karachi and high over Lahore and Gandhi College. The results suggest the high number of PCs only over Lahore. In summer season, the high number i.e., 74 % of the total data counts over Gandhi College are identified as cloudy days, 60 % of which are PCs. Similarly, most of the clouds over Lahore, Delhi and Jaipur are PCs. Conversely, the least number of PCs (6 %) are found over Karachi.

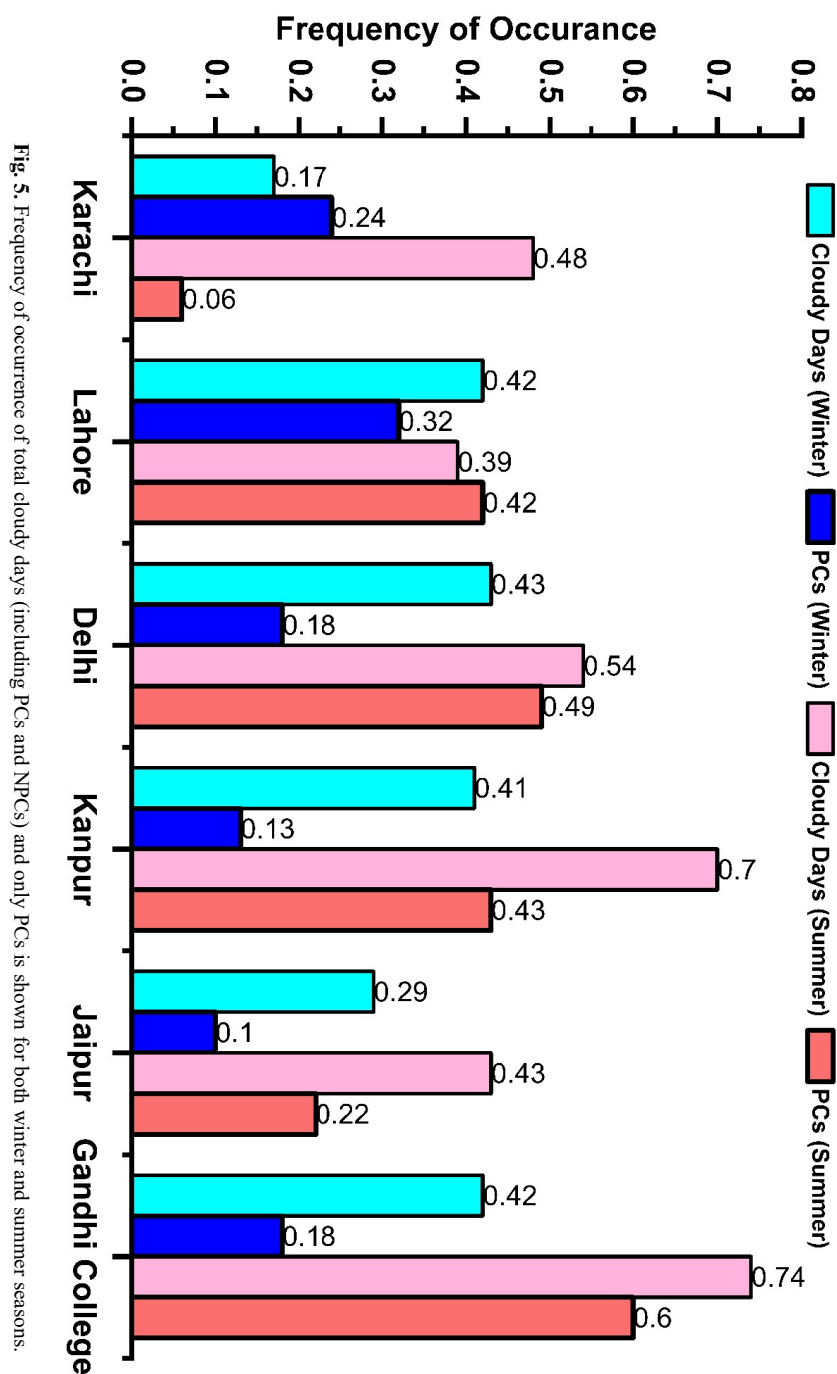




Table 3 shows the criteria adopted from previous papers (Rossow & Schiffer, 1999; Wyant et al., 2006; Sharma et al., 2023) for further classification of NPCs and PCs into different type of clouds. The aim of identifying the cloud types is to assess the cloud regimes and their vertical structure for a better understanding of ACPI. In accordance with table 3, Fig. 6 shows joint histograms of COT-CTP displaying the mean CF values for nine different types of clouds. For a quick visual comparison, the cloud types are ordered from low to high level clouds. Also, for each histogram, the bins of COT and CTP are located on x- and y-axis respectively. While the CF of each bin is represented with the colored bar with its value mentioned in the histograms as shown in Fig. 6.

The results exhibit noticeable differences in the pattern of cloud regimes over all study areas. The diverse CF values are observed in winter and summer seasons for NPCs and PCs over Karachi. In winter season, only stratus NPCs ($23 < \text{COT} < 60$, $\text{CTP} > 680$ hPa) are dominant ($\text{CF} \geq 0.7$). While, in summers, meaningful CF values for thick clouds such as stratus, nimbo-stratus and deep convective NPCs ($0 < \text{COT} < 60$, $180 < \text{CTP} < 440$ hPa) are observed. Similarly, in winter season the type of PCs includes thick nimbo- and alto-stratus and deep convective clouds. While, in summers only high-level thin cirrus clouds have high CF values. The relatively reduced value of CF for thick NPCs in winters and PCs in summers is attributed to the low values of AOD and high values of LTS. The results depicted slight differences and similarities in CF values for thick and thin NPCs respectively in winter season for all areas except Karachi. Besides, the high-level PCs are identified in one bin of CTP ($180 < \text{CTP} < 440$ hPa) over all study areas. The formation of these similar types of PCs in winters are associated with the similarities in Ω , LTS values and aerosols concentration.

Also, in summer season, the matrices of PCs and NPCs exhibit a wide range of cloud types. However, the CF values are comparatively high for PCs. The results suggest less significant values for the low-lying thick NPCs over Lahore. Moreover, the results illustrate a more frequent occurrence of all the three types of thick NPCs in one bin of COT ($23 < \text{COT} < 60$) and all the three types of high-level NPCs for CTP ($180 < \text{CTP} < 440$ hPa) over Delhi, Kanpur, Jaipur and Gandhi College. Therefore, these are considered the cloudiest regimes. Besides, contrasting regional variations are also observed in PCs. The largest CF values for all types of PCs are observed over Kanpur and Gandhi College. Similarly, relatively good values of CF in a bin of COT ($23 < \text{COT} < 60$) and a bin of CTP ($180 < \text{CTP} < 440$ hPa) over Lahore, Delhi, and Jaipur depict the frequent occurrence of thick and high-level PCs respectively. In addition,



among all the estimated low-level PCs, only stratus clouds exhibit good CF values over all areas except Karachi. The formation of thick and high-level clouds can be attributed to the enhanced convection process due to the atmospheric instability.

Table 3. Classification of clouds based on CTP – COT joint histograms.

CTP (hPa)	COT		
	0-3.6	3.6-23	23 to >60
440 to <180	Cirrus	Cirr-Stratus	Deep convection
680-440	Alto-Cumulus	Alto-Stratus	Nimbo-Stratus
>800 to 680	Cumulus	Strato-Cumulus	Stratus

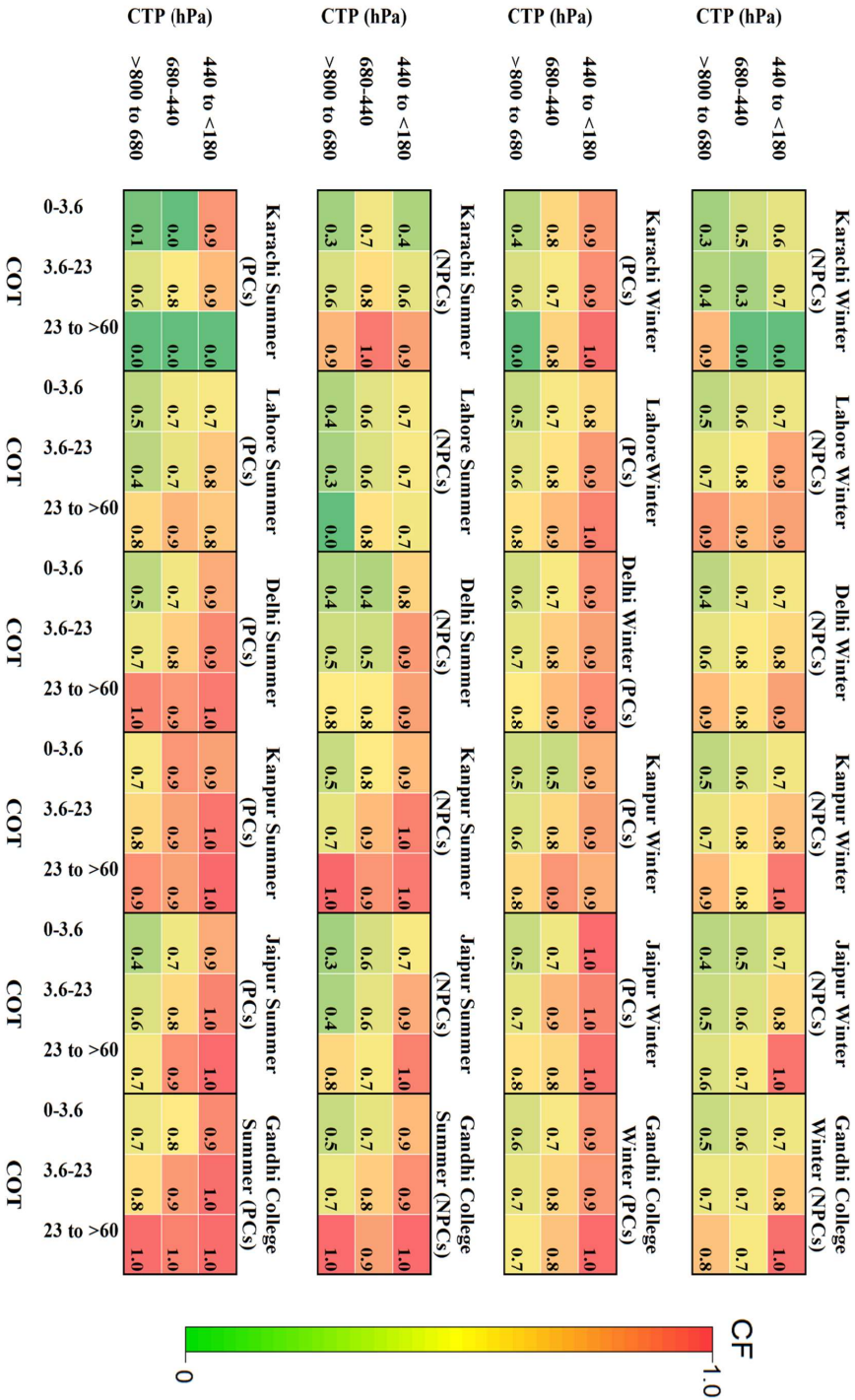


Fig. 6. Types of NPCs and PCs in winter and summer season



After estimating the cloud types, Fig. 7 shows the probability distribution function (PDF) of cloud microphysical properties for the identification of differences in microstructure of NPCs and PCs in summer and winter seasons. From the results it is depicted an approximately similar pattern for the CER of NPCs in winter. However, the clouds have high peaks of PDF for lower values of CDNC over Karachi. The low number of CDNC results in thin NPCs as shown in Fig.6. Similarly, Fig. 7(c and g) shows the microstructure of NPCs in summer. The results indicate that as compared to CER values in winter, the probability of $CER > 15 \mu m$ is high in summer season. However, high peak for $CER < 15 \mu m$ is observed over Karachi. Similarly, the CDNC shows a high probability for $CDNC > 50 cm^{-3}$ with the high PDF values over Karachi. Where, the lowest number of CDNC is observed over Lahore indicating the formation of high-level thin NPCs in summer.

Fig. 7(b and f) shows the distribution pattern of CER and CDNC of PCs in winter season. It is clearly observed that the distribution of CER for PCs is like those for NPCs in winter season. However, PDF has peak values for relatively higher CDNC, which illustrates the occurrence of thick clouds. Fig. 7(d and h) shows the variations in CER and CDNC in summer season. The results show a wider distribution for $CER > 15 \mu m$ and higher peaks for $CDNC > 50 cm^{-3}$ suggesting the formation of thick PCs in summer as shown in Fig.6.

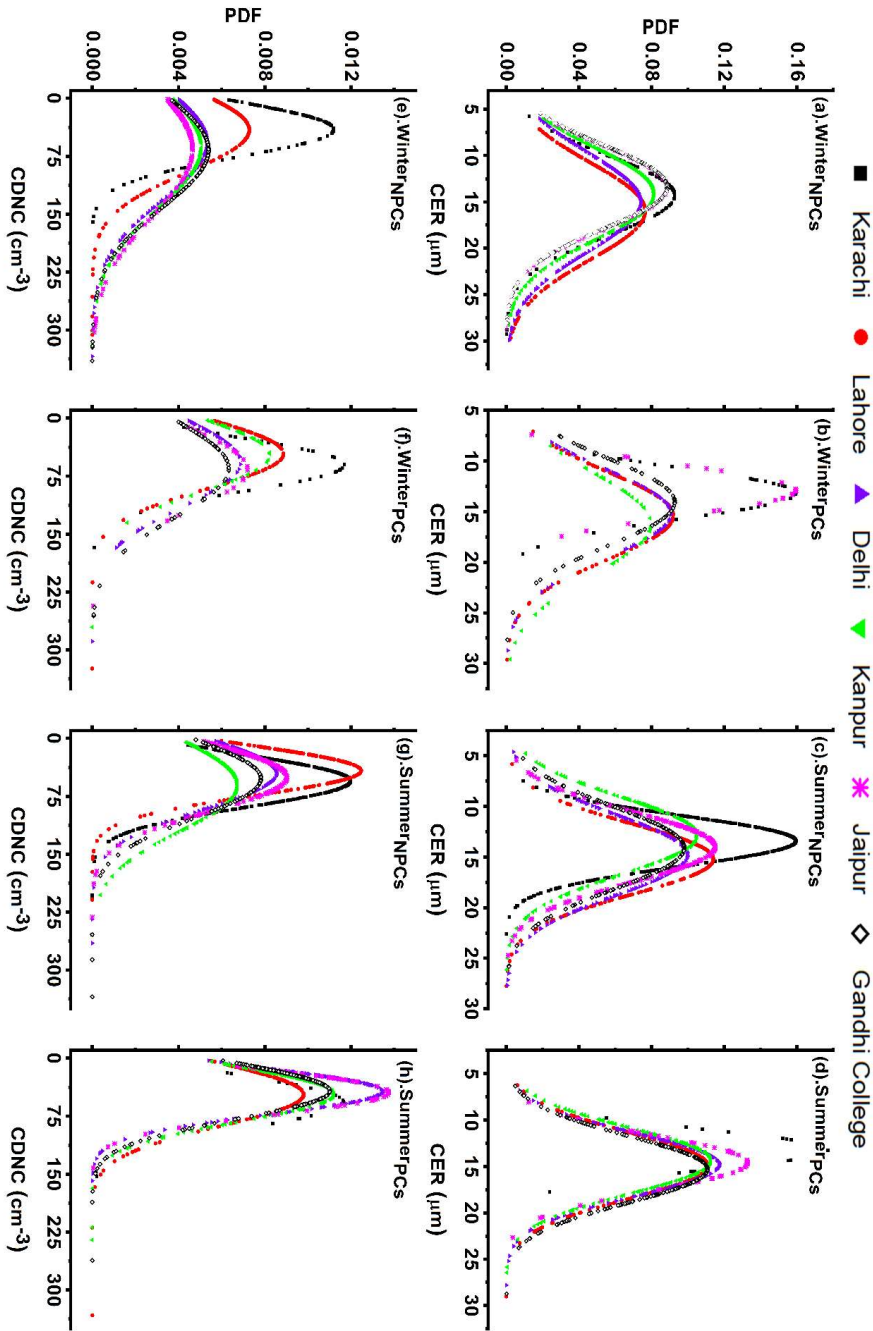


Fig. 7. Probability density function (PDF) of precipitating (PCs) and non-precipitating clouds (NPCs) in winter and summer season



3.4. Aerosol-Cloud-Precipitation Interaction (ACPI)

In the following sections, ACPI is analyzed and discussed in detail for PCs and NPCs in summer and winter seasons.

3.4.1. *Aerosol effects on cloud properties*

The impact of aerosols on CDNC and CER of PCs and NPCs is illustrated as scatter plots in Fig. 8-9. The quantification of the AOD-CER and AOD-CDNC relationships is demonstrated through detailed linear regressed slopes, regression coefficients (R^2) and Pearson's correlation coefficient (R). The color bar represents the variations in LTS. Fig.8 shows that in winter season, the AOD-CER correlation is good for PCs and weak for NPCs. The results also show that the LTS values are higher for NPCs. The weak AOD-CER correlation may be linked to the inhibition of droplet growth due to less soluble aerosols, originated from biomass burning (Kang et al., 2015). In our case, all the selected study areas are among the most urbanized and industrialized areas of IGP. Therefore, most of the prevailing aerosols are the less soluble soot and BC particles. That weakened activation of cloud droplets inhibits the formation of PCs and evaporate to higher altitudes and thereby increases the droplet residence time (Kumar & Physics, 2013). Besides, the results show a contrasting pattern of LTS values. Although, RH over Karachi ($38.3 \pm 9\%$) is higher than over the other study areas (shown in Table 2), the negative AOD-CER correlation is observed over Karachi due to its coastal location, the low value of AOD and high level of LTS.

Fig. 9 illustrates the AOD-CER and AOD-CDNC correlation in summer season. The results depict a more significant and positive AOD-CER correlation in summer season than winter season. Unlike winter season, the high LTS values are observed for PCs. Yuan(2008) associated the positive AOD-CER correlation to the soluble organic aerosols. Myhre et al. (2007) hypothesized that the positive AOD-CER correlation is a maximum for low CTP and minimum for high CTP. Hence, in our study, referable to the approximated CF values shown in Fig.6, the significant and positive AOD-CER correlation under unstable atmospheric conditions resulted in thick and high-level clouds. Furthermore, it is observed that CER and CDNC values for NPCs increase with increasing instability. Meanwhile, the enhanced process of droplet activation may result in large AOD, higher CER, giant and fewer CCN (Yuan, 2008). Therefore, the weak correlation of AOD with CER and CDNC may be due to the anthropogenically ejected water-soluble organic aerosols and a smaller number of CCN.

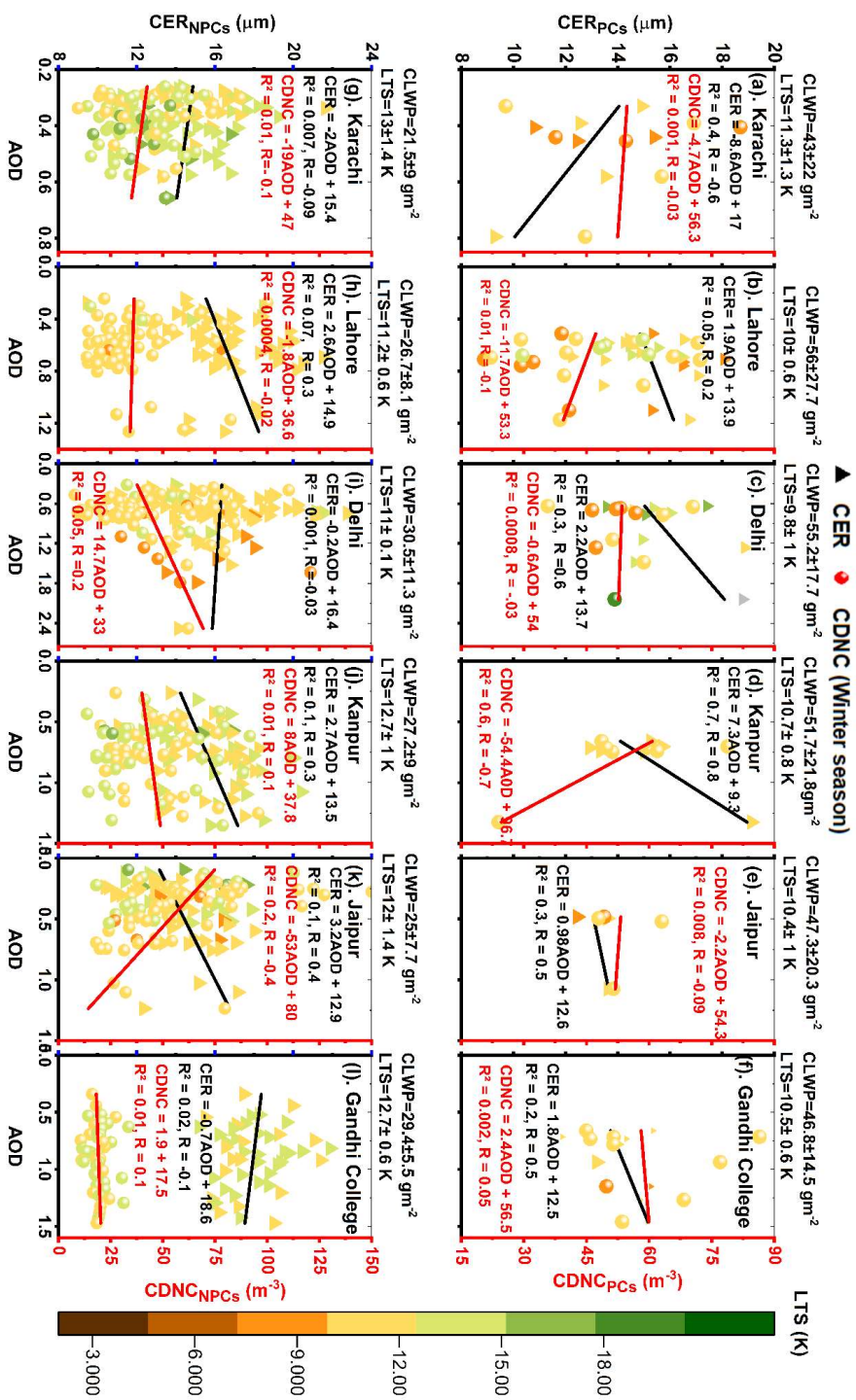


Fig. 8. AOD-CER and AOD-CDNC regression and correlation coefficient for PCs and NPCs over all study areas in winter season.

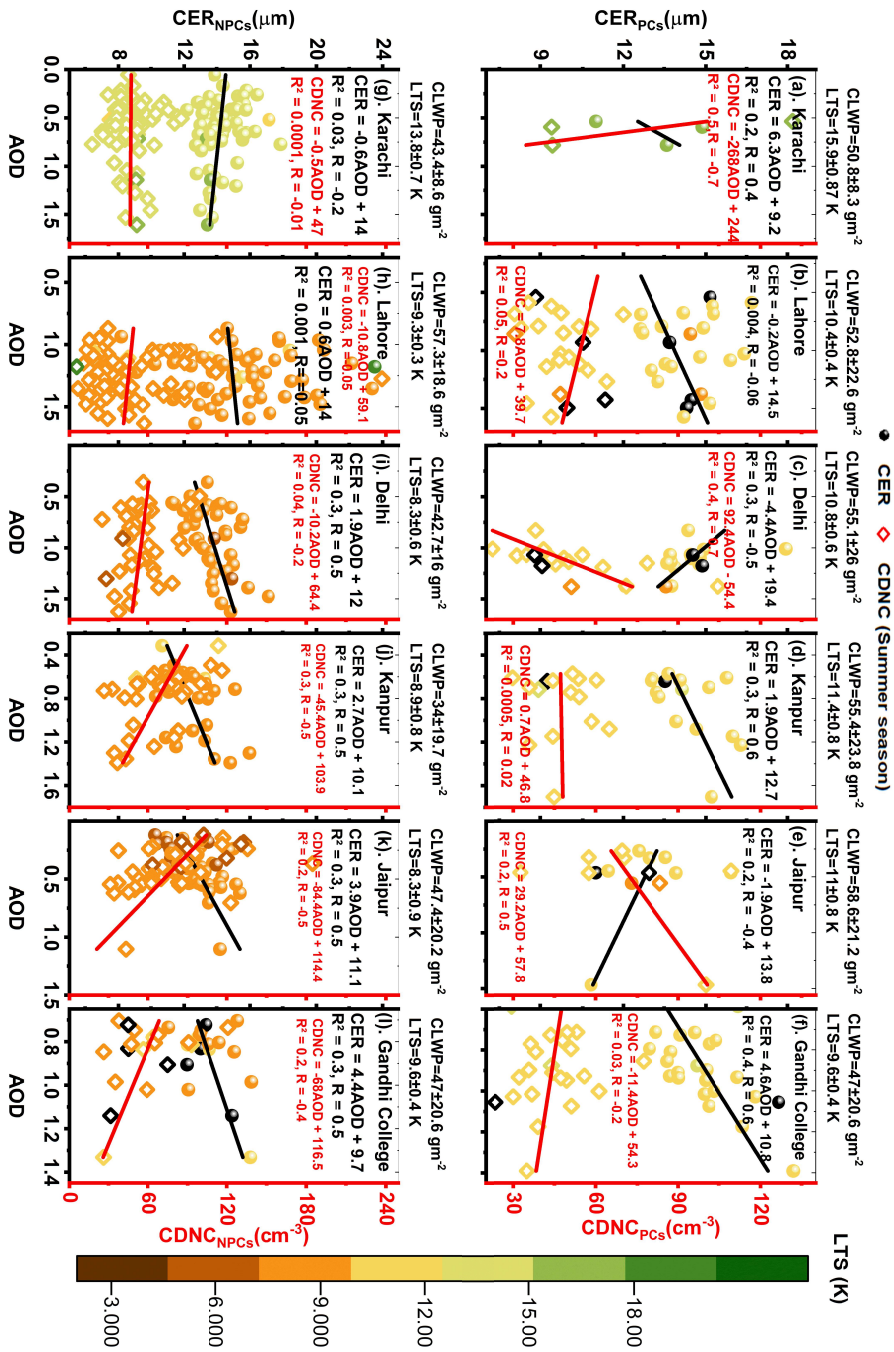


Fig. 9. Same as Fig. 8 but in summer season.



3.4.2. Seasonal variations in sensitivities of aerosol-cloud indirect effects and ACI

Fig.10 shows assessment of four ACI sensitivities in terms of CDNC using daily mean values of MODIS observations available over the entire study area. Since studying the effects of aerosols on the co-located clouds is a challenging task due to the overestimation of thin clouds in AOD retrievals. Therefore, to minimize the propagation of AOD retrieval errors in ACI, the current study attempted to estimate the sensitivities of different cloud mechanisms to CDNC.

The sensitivity of CER to CDNC is assessed as a signature of FIE as shown in Fig.10a. The positive values illustrate that CER decreases with an increase in CDNC revealing the occurrence of the Twomey effect. Whilst the negative values depict the anti-Twomey effect. The approximations in winter season show strong (weak) sensitivity of FIE for PCs (NPCs). Similarly, the estimated sensitivity of FIE for all NPCs and PCs is also positive in the summer season.

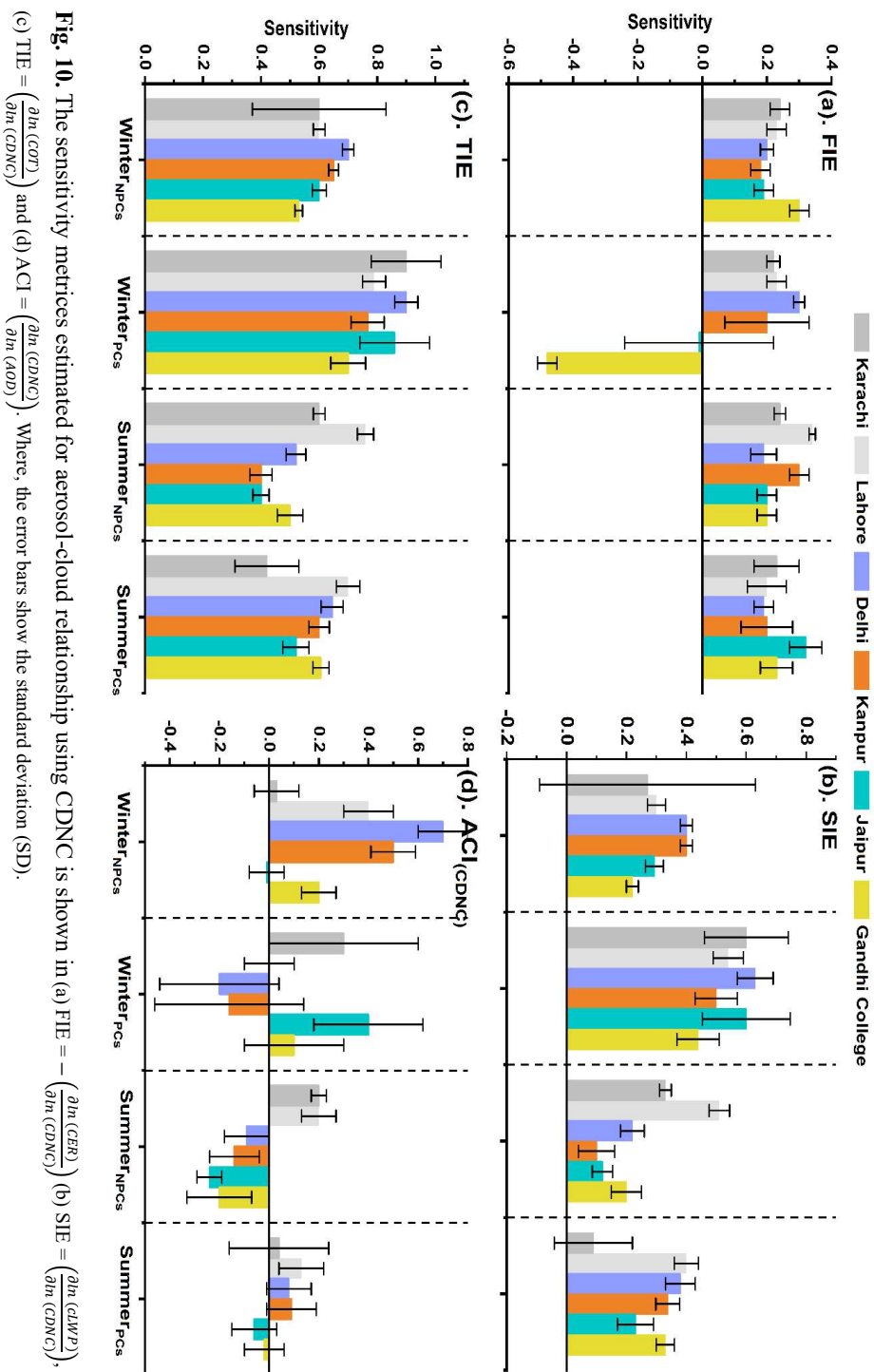
Fig. 10b illustrates the sensitivity of CLWP to CDNC as a proxy for evaluation of the SIE or lifetime effect. The positive sensitivity estimated for all NPCs and PCs suggested that the CLWP increased with increase in aerosol. Further, the results show that the sensitivity of SIE is stronger for PCs in winter which indicates the delay and onset of high PR. Similarly, the results show that the SIE sensitivity values are higher for PCs than for NPCs in the corresponding seasons. Therefore, the results depict that the lifetime of PCs is greater than NPCs. Which is attributed to the high level of RH for PCs as shown in Table 2. Fig. 10 (a and b) shows that the FIE sensitivities are weaker than SIE.

Fig. 10c shows the TIE in terms of the sensitivity of COT to CDNC. The results illustrate positive values of sensitivity for all NPCs and PCs which indicate that COT increases with increase in aerosol concentration. The results also reveal that sensitivity of TIE is a linear sum of the sensitivities of FIE and SIE. Further, the results also suggest that the variations in TIE sensitivity are largely dependent on SIE.

Fig.10d shows the sensitivity of CDNC to AOD as an estimation of ACI in terms of CDNC. The positive values show the increase in CDNC with the increase in AOD. Therefore, positive ACI reflects the inhibition of precipitation formation. Whilst the negative values illustrate the decrease in CDNC and enhanced PR (Fan et al., 2018). The results depicted relatively large and positive sensitivities for NPCs in winter over Lahore, Delhi, and Kanpur, which inhibits the onset of rainfall. The Sensitivity of ACI for NPCs in summer is positive over Karachi and



Lahore and negative over Delhi, Kanpur, Jaipur, and Gandhi College. Ackerman et al. (2004) associated the negative ACI_{CDNC} to the wet scavenging and mixing of air by entrainment. In our case, negative ACI may be due to the growth of CER and decrease in CDNC with aerosol loading under unstable conditions (shown in Fig. 9). Further, the magnitude of sensitivity for PCs in summer is low. Which can be due to the droplet growth through collision coalescence and wet scavenging in thick clouds, decreased dependency on CCN.





3.4.3. Aerosol effects on precipitation

Fig. 11 shows the average values of PR in mm/day retrieved from TRMM. The results show an obvious seasonal difference in precipitation occurrence. The reason for the high (low) PR values is due to the suitable meteorological condition including high (low) LTS values for PCs in summer (winter) season (shown in Fig. 8-9). The results show high (low) approximation of PR over Gandhi College (Karachi). Knowing that the rate of conversion of CDNC to precipitation is proportional to CER (Wolf & Toon, 2014). Therefore, the high PR values is due to the growth of bigger cloud droplets in summers. Further, apart from the reasons mentioned in the preceding sections, the other justification for the differently perturbed aerosols, clouds and precipitation pattern over the study areas in summers is due to the entrance of southwest winds from Bay of Bengal passing across Gandhi College to Delhi and Lahore and entrance of same winds from Arabian sea to Pakistan through Karachi (Anwar et al., 2022).

Fig. 12 shows scatter plots of PR verses CDNC. The plot is colored with COT to examine the impact of CDNC on PR for similar macrophysics. When CDNC are few, then the CER are sparse that grow larger, form less reflective clouds and precipitate faster (Kump & Pollard, 2008). The same phenomenon seems true in our case. The results illustrate high PR values for comparatively thin clouds with fewer CDNC (i.e., $CDNC < \sim 50 \text{ cm}^{-3}$) and intermediate for optically thick clouds and $CDNC > \sim 50 \text{ cm}^{-3}$.

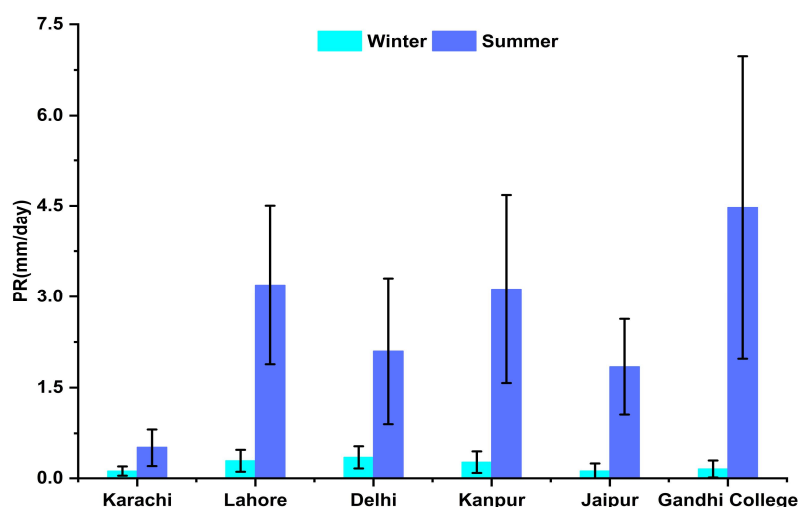


Fig. 11. Precipitation rate (PR) for the PCs in winter and summer season. The error bars show the SD values with 95% confidence interval.

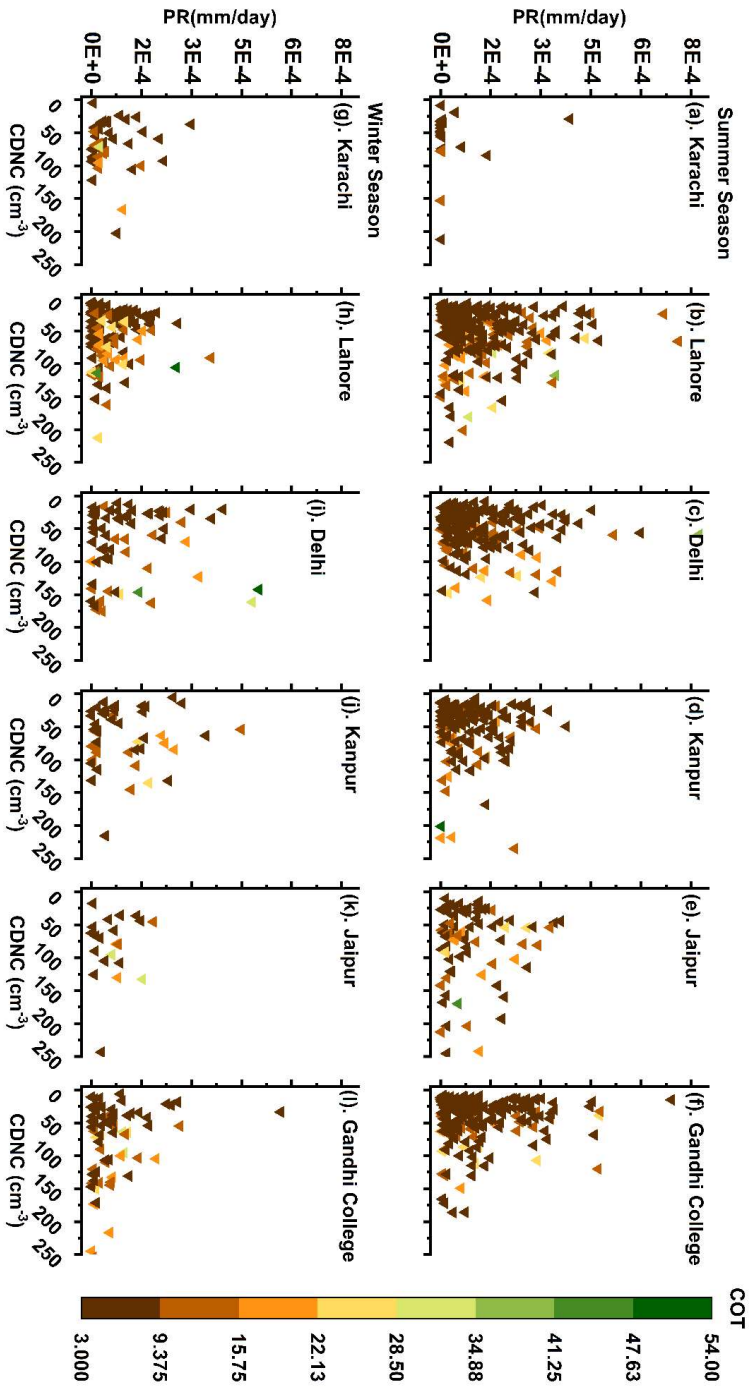


Fig. 12. Scatter diagrams of PR (mm/day) versus CDNC (cm^{-3}) in summer and winter seasons. color coding shows the COT of PCs.



Fig.13 shows the sensitivity (S_o) of PR to CDNC defined by $S_o = \left(-\frac{d\ln(PR)}{d\ln(CDNC)} \right)_{COT}$ for clouds of low and intermediate thickness illustrated in Fig. 13 a and Fig. 13 b respectively. However, sensitivity analysis for $COT > 23$ could not be performed due to smaller number of available samples. In the sensitivity equation the minus sign shows the suppression of precipitation formation due to the increase in CDNC. Further, when S_o is positive, correlation between PR and CDNC is negative; however, for negative S_o , PR and CDNC are positively correlated. The results show peak values of S_o at intermediate values of COT in winter, indicating the occurrence of lightly precipitating clouds. Referring to Fig. 13b, the low magnitude of S_o is due to coagulation, in which precipitations are less sensitive to CDNC.

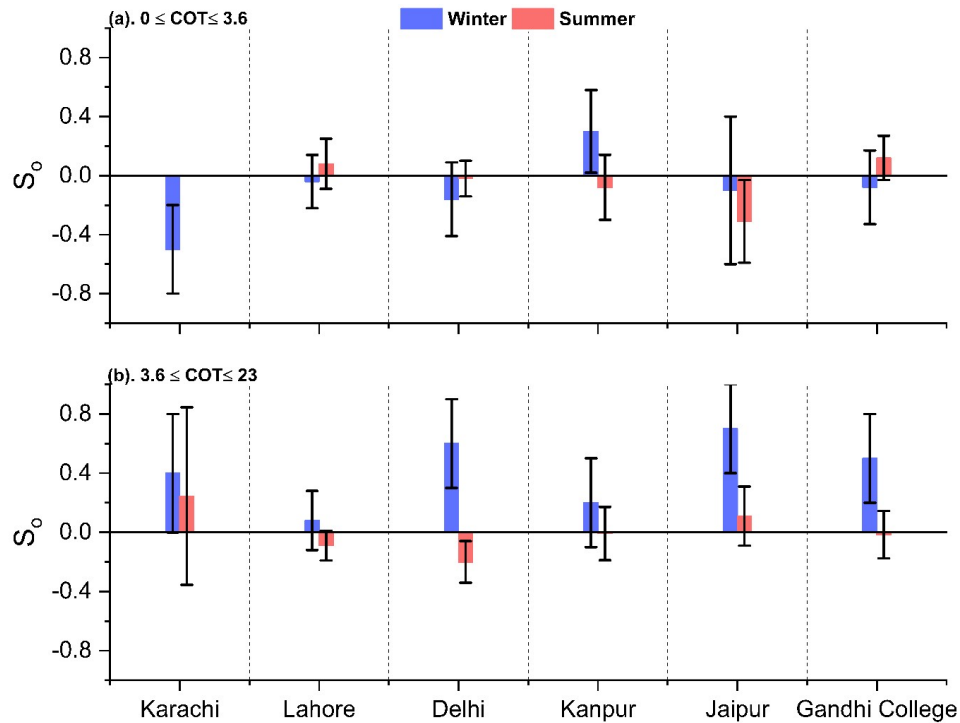


Fig. 13. Sensitivity ‘ S_o ’ of precipitation rate (PR) for two bins of COT shown in (a). $0 \leq COT \leq 3.6$ and (b). $3.6 \leq COT \leq 23$.



4. Conclusion

In this study, the long-term (2001-2021) data retrievals from MODIS coupled with TRMM and NCEP/NCAR reanalysis-II datasets over the entire study area are compiled and analyzed for PCs and NPCs in winter and summer season. The following are the main findings of this study.

A decadal decrease in AOD is observed over Karachi (-1.9%) and Jaipur (-0.5%). Meanwhile, AOD exhibits an increase over Lahore (5.2%), Delhi (9%), Kanpur (10.7%) and Gandhi College (22.7%). The LTS values are High (low) for NPCs (PCs) in winter and for PCs (NPCs) in summer season. However, among all study areas, Karachi exhibits comparatively high LTS values in both seasons. Apart from that, the increase in RH% for PCs ranged from 33-57% in winter and from 25-45 % in summer. $\Omega > 0$ for all NPCs in winter and < 0 for PCs in both winter and summer seasons.

In winter season low frequency of cloudy days over Karachi and high over Lahore and Gandhi College is estimated. Also, the high number of PCs are estimated only over Lahore. In summer season, out of the 74 % of the cloudy days, 60 % are PCs over Gandhi College. Similarly, most of the clouds over Lahore, Delhi and Jaipur are PCs. Conversely, the least number of PCs (6 %) is found over Karachi. The high-level PCs are identified in one bin of CTP ($180 < \text{CTP} < 440$ hPa) over all study areas in winters. In summer season, all the three types of high level and thick PCs have meaningful CF values. Also, the frequently occurred low level PCs are approximated as stratus clouds. Further, PDF values for CER $> \sim 15 \mu\text{m}$ and CDNC $> \sim 50 \text{cm}^{-3}$ for NPCs and PCs is high in summer and lower in winter over all areas except Karachi.

The AOD-CER correlation is good for PCs and weak for NPCs in winter season. Also, the CER and CDNC values increase with increase in LTS. The sensitivity value of FIE is high (low) for PCs (NPCs) in winter. Further, magnitude of sensitivity of FIE (SIE) is low (high). Also, the sensitivity of TIE is a linear sum of the sensitivities of FIE and SIE. Further, ACI sensitivity values for PCs in summer are small, illustrating less dependency of CER on CDNC in thick clouds.

The high (low) PR values are observed in summer (winter). Further, high PR values for comparatively thin clouds with fewer CDNC $< \sim 50 \text{cm}^{-3}$ and intermediate for optically thick clouds and CDNC $> \sim 50 \text{cm}^{-3}$ are observed. Sensitivity values are small (high) for thick clouds in summer (winter).



Being one of the major source regions of anthropogenic aerosols across the globe, IGP offers interesting insights into the study of ACPI coupled with aerosol indirect effects. This study highlights that the aerosol-cloud relationship exhibits different behavior under different meteorological conditions, at coastal and inland locations. Thus, compared to other study areas, the stable atmospheric conditions due to the constant sea breeze weakened the ACI over Karachi, which resulted in a smaller number of CDNC, NPCs, and PCs. Further, our study also provides a very good platform for the detailed analysis of sensitivity tests of aerosol indirect effects and precipitation formation.

Limitations and future recommendations:

Although, the scope of this study is limited to satellite-based analysis of aerosol-cloud-precipitation interaction (ACPI) and indirect effects due to the lack of in-situ measuring instruments in Pakistan, and the intrinsic uncertainties associated with satellite-based data. Therefore, simulations of ground-based measurements along with satellite-based retrievals and calculation of cloud properties and CCN by different Community Atmosphere Model (CAM) and Weather Research and Forecasting (WRF) Models are recommended for deep insight into the various mechanisms of ACPI over complex topography of IGP.

Data Availability: The MODIS and TRMM data can be obtained from the NASA Goddard Earth Sciences Data and Information Center (GES DISC) and can be retrieved from the websites: <https://ladsweb.modaps.eosdis.nasa.gov/missions-and-measurements/products/13-atmosphere/> and <https://gpm.nasa.gov/data>. The reanalysis-II datasets are obtained from the website: <https://psl.noaa.gov/data/gridded/data.ncep.reanalysis2.html>. The processed data used in this work are available on reasonable request from the corresponding author.

Author contribution: NG processed and analyzed the data and wrote the original draft of the manuscript. KA proposed the Idea, supervised this work and revised the manuscript. YL helped in revising the manuscript.

Competing Interest: The authors declare that they have no conflict of interest.

Acknowledgment: The authors gratefully acknowledge the NASA Goddard Earth Sciences Data and Information Services Center (GES DISC) for the provision of freely available data retrieved from MODIS and TRMM. We are also grateful to the NOAA Physical Sciences Laboratory (PSL) for free accessibility to (NCEP/NCAR) reanalysis-II datasets.



References

- Ackerman, A. S., Kirkpatrick, M. P., Stevens, D. E., & Toon, O. B.: The impact of humidity above stratiform clouds on indirect aerosol climate forcing, *Nature.*, *432*, 1014-1017, doi:10.1038/nature03174, 2004.
- Alam, K., Iqbal, M. J., Blaschke, T., Qureshi, S., & Khan, G. J. A. i. S. R. : Monitoring spatio-temporal variations in aerosols and aerosol–cloud interactions over Pakistan using MODIS data, *Adva. Space Res.*, *46*, 1162-1176, <https://doi.org/10.1016/j.asr.2010.06.025>, 2010.
- Alam, K., Qureshi, S., & Blaschke, T. J. A. e.: Monitoring spatio-temporal aerosol patterns over Pakistan based on MODIS, TOMS and MISR satellite data and a HYSPLIT model, *Atmos. Envi.*, *45*, 4641-4651, <https://doi.org/10.1016/j.atmosenv.2011.05.055>, 2011.
- Albrecht, B. A. J. S.: Aerosols, cloud microphysics, and fractional cloudiness, *Sci.*, *245*, 1227-1230, <https://doi.org/10.1126/science.245.4923.122>, 1989
- Andreae, M., & Rosenfeld, D. J. E.-S. R.: Aerosol–cloud–precipitation interactions. Part 1. The nature and sources of cloud-active aerosols, *Earth. Sci. Rev.*, *89*, 13-41, <https://doi.org/10.1016/j.earscirev.2008.03.001>, 2008.
- Anttila, T., Brus, D., Jaatinen, A., Hyvärinen, A. P., Kivekäs, N., Romakkaniemi, S., ... & Lihavainen, H.: Relationships between particles, cloud condensation nuclei and cloud droplet activation during the third Pallas Cloud Experiment, *Atmos. Chem. Phys.*, *12*, 11435-11450, <https://doi.org/10.5194/acp-12-11435-2012>, 2012.
- Anwar, K., Alam, K., Liu, Y., Huang, Z., Huang, J., & Liu, Y. J. A. R.: Analysis of aerosol cloud interactions with a consistent signal of meteorology and other influencing parameters, *Atmos. Res.*, *275*, 106241, <https://doi.org/10.1016/j.atmosres.2022.106241> , 2022.
- Brenguier, J.-L., Pawlowska, H., Schüller, L., Preusker, R., Fischer, J., & Fouquart, Y. J. J. o. t. a. s.: Radiative properties of boundary layer clouds: Droplet effective radius versus number concentration, *Atmos. Sci.*, *57*, 803-821, [https://doi.org/10.1175/1520-0469\(2000\)057<0803:RPOBLC>2.0.CO;2](https://doi.org/10.1175/1520-0469(2000)057<0803:RPOBLC>2.0.CO;2) , 2000.
- Chen, Q., Yin, Y., Jin, L.-j., Xiao, H., & Zhu, S.-c. J. A. r.: The effect of aerosol layers on convective cloud microphysics and precipitation, *Atmos. Res.*, *101*, 327-340, <https://doi.org/10.1016/j.atmosres.2011.03.007>, 2011
- Costantino, L., & Bréon, F. M. J. G. R. L.: Analysis of aerosol-cloud interaction from multi-sensor satellite observations, *Atmos. Sci.*, *37*, <https://doi.org/10.1029/2009GL041828> ,2010



- Fan, C., Ding, M., Wu, P., & Fan, Y. J. a. p. a.: The Relationship between Precipitation and Aerosol: Evidence from Satellite Observation, *Atmos. Oce. Phy.*, <https://doi.org/10.48550/arXiv.1812.02036>, 2018.
- Feingold, G., Eberhard, W. L., Veron, D. E., & Previdi, M. J. G. R. L.: First measurements of the Twomey indirect effect using ground-based remote sensors, *Geophys. Res. Lett.*, *30*, <https://doi.org/10.1029/2002GL016633>, 2003.
- Gryspeerd, E., Quaas, J., & Bellouin, N.: Constraining the aerosol influence on cloud fraction, *JGR. Atmos.*, *121*, 3566-3583, <https://doi.org/10.1002/2015JD023744>, 2016.
- Jiang, H., Feingold, G., & Cotton, W. R. J. J. o. G. R. A.: Simulations of aerosol-cloud-dynamical feedbacks resulting from entrainment of aerosol into the marine boundary layer during the Atlantic Stratocumulus Transition Experiment, *JGR. Atmos.*, *107*, AAC 20-1-AAC 20-11, <https://doi.org/10.1029/2001JD001502>, 2002.
- Jung, E.: Aerosol-cloud-precipitation interactions in the trade wind boundary layer, Ph.D Thesis, Meteorology and Physical Oceanography, University of Miami, 91-pp., 2012.
- Kang, N., Kumar, K. R., Yin, Y., Diao, Y., Yu, X. J. A., & Research, A. Q.: Correlation analysis between AOD and cloud parameters to study their relationship over China using MODIS data (2003-2013): impact on cloud formation and climate change, *AAQR.*, *15*, 958-973, <https://doi.org/10.4209/aaqr.2014.08.0168>, 2015.
- Kaskaoutis, D. G., Kumar Kharol, S., Sinha, P., Singh, R. P., Kambezidis, H., Rani Sharma, A.: Extremely large anthropogenic-aerosol contribution to total aerosol load over the Bay of Bengal during winter season, *Atmos. Chem. Phys.*, *11*, 7097-7117, <https://doi.org/10.5194/acp-11-7097-2011>, 2011.
- Kedia, S., Ramachandran, S., Holben, B. N., & Tripathi, S. J. A. E.: Quantification of aerosol type, and sources of aerosols over the Indo-Gangetic Plain, *Atmos. Environ.*, *98*, 607-619, <https://doi.org/10.1016/j.atmosenv.2014.09.022>, 2014.
- Koike, M., Asano, N., Nakamura, H., Sakai, S., Nagao, T., & Nakajima, T. J. J. o. G. R. A.: Modulations of aerosol impacts on cloud microphysics induced by the warm Kuroshio Current under the East Asian winter monsoon, *JGR. Atmos.*, *121*, 282-297, <https://doi.org/10.1002/2016JD025375>, 2016.
- Kubar, T. L., Hartmann, D. L., & Wood, R. J. J. o. t. a. s.: Understanding the importance of microphysics and macrophysics for warm rain in marine low clouds. Part I: Satellite observations, *Atmos. Sci.* *66*, 2953-2972, <https://doi.org/10.1175/2009jas3071.1>, 2009.



- Kumar, A. J. J. o. A., & Physics, S.-T.: Variability of aerosol optical depth and cloud parameters over North Eastern regions of India retrieved from MODIS satellite data, *Atmos. Sol. Terr. Phys.*, *100*, 34-49, <https://doi.org/10.1016/j.jastp.2013.03.025>, 2013.
- Kump, L. R., & Pollard, D.: Amplification of Cretaceous Warmth by Biological Cloud Feedbacks, *Sci.*, *320*, 195-195, <https://doi.org/10.1126/science.1153883>, 2008.
- Li, J., Lv, Q., Zhang, M., Wang, T., Kawamoto, K., Chen, S., & Zhang, B.: Effects of atmospheric dynamics and aerosols on the fraction of supercooled water clouds, *Atmos. Chem. Phys.*, *17*, 1847-1863, <https://doi.org/10.5194/acp-17-1847-2017>, 2017.
- Masmoudi, M., Chaabane, M., Tanré, D., Gouloup, P., Blarel, L., & Elleuch, F. J. A. R.: Spatial and temporal variability of aerosol: size distribution and optical properties, *Atmos. Res.*, *66*, 1-19, [https://doi.org/10.1016/S0169-8095\(02\)00174-6](https://doi.org/10.1016/S0169-8095(02)00174-6), 2003.
- McCoy, D. T., Field, P. R., Schmidt, A., Grosvenor, D. P., Bender, F. A. M., Shipway, B. J., ... & Elsaesser, G. S.: Aerosol midlatitude cyclone indirect effects in observations and high-resolution simulations, *Atmos. Chem. Phys.*, *18*, 5821-5846, <https://doi.org/10.5194/acp-18-5821-2018>, 2018.
- Michibata, T., Kawamoto, K., & Takemura, T. J. A. C. P. D.: The effects of aerosols on water cloud microphysics and macrophysics based on satellite observations over East Asia and the North Pacific, *Atmos. Chem. Phys.*, *14*, 10515-10541, <https://doi.org/10.5194/acp-14-11935-2014>, 2014.
- Myhre, G., Stordal, F., Johnsrud, M., Kaufman, Y., Rosenfeld, D., Storelvmo, T., . . . Physics.: Aerosol-cloud interaction inferred from MODIS satellite data and global aerosol models, *Atmos. Chem. Phys.*, *7*, 3081-3101, <https://doi.org/10.5194/acp-7-3081-2007>, 2007.
- Naud, C. M., Posselt, D. J., & van den Heever, S. C.: Observed covariations of aerosol optical depth and cloud cover in extratropical cyclones, *JGR: Atmos.*, *122*, 10-338, <https://doi.org/10.1002/2017JD027240>, 2017.
- Rossow, W. B., & Schiffer, R. A. J. B. o. t. A. M. S.: Advances in understanding clouds from ISCCP, *Bul. Americ. Meteor. Soci.*, *80*, 2261-2288, [https://doi.org/10.1175/15200477\(1999\)080<2261:AIUCFI>2.0.CO;2](https://doi.org/10.1175/15200477(1999)080<2261:AIUCFI>2.0.CO;2), 1999.
- Sharma, P., Ganguly, D., Sharma, A. K., Kant, S., Mishra, S. J. E., & Science, S.: Assessing the aerosols, clouds and their relationship over the northern Bay of Bengal using a global climate model, *Earth. Spac. Sci.*, *10*, e2022EA002706, <https://doi.org/10.1029/2022EA002706>, 2023.



- Singh, A., Rastogi, N., Sharma, D., Singh, D. J. A., & Research, A. Q.: Inter and intra-annual variability in aerosol characteristics over northwestern Indo-Gangetic Plain, AAQR., *15*, 376-386, <https://doi.org/10.4209/aaqr.2014.04.0080>, 2015.
- Srivastava, P., Pal, D. K., Aruche, K. M., Wani, S. P., & Sahrawat, K. L. J. E.-S. R.: Soils of the Indo-Gangetic Plains: a pedogenic response to landscape stability, climatic variability and anthropogenic activity during the Holocene, *Earth. Sci. Rev.*, *140*, 54-71, <https://doi.org/10.1016/j.earscirev.2014.10.010>, 2015.
- Tao, W.-K., Chen, J.-P., Li, Z., Wang, C., & Zhang, C.: Impact of aerosols on convective clouds and precipitation, *Rev. Geophys.*, *50*, <https://doi.org/10.1029/2011RG000369>, 2012.
- Thomas, A., Kanawade, V. P., Sarangi, C., & Srivastava, A. K. J. S. o. t. T. E.: Effect of COVID-19 shutdown on aerosol direct radiative forcing over the Indo-Gangetic Plain outflow region of the Bay of Bengal, *Sci. Total Envi.*, *782*, 146918, <https://doi.org/10.1016/j.scitotenv.2021.146918>, 2021.
- Twomey, S. J. J. o. t. a. s.: The influence of pollution on the shortwave albedo of clouds, *Atmos. Sci.*, *34*, 1149-1152, [https://doi.org/10.1175/1520-0469\(1977\)034<1149:TIOPOP>2.0.CO;2](https://doi.org/10.1175/1520-0469(1977)034<1149:TIOPOP>2.0.CO;2), 1977.
- Verma, S., Ramana, M. V., & Kumar, R. J. S. r.: Atmospheric rivers fueling the intensification of fog and haze over Indo-Gangetic Plains, *Sci. Reports.*, *Nature*, *12*, 5139, 2022.
- Wolf, E., & Toon, O. J. A.: Controls on the Archean climate system investigated with a global climate model, *Astrobiology*, *14*, 241-253, <https://doi.org/10.1089/ast.2013.1112>, 2014.
- Wood, R. J. U. o. W.: Relationships between optical depth, liquid water path, droplet concentration, and effective radius in adiabatic layer cloud, *University of Washington*, *3*, 2006.
- Wu, P., Dong, X., Xi, B., Liu, Y., Thieman, M., & Minnis, P. J. J. o. G. R. A.: Effects of environment forcing on marine boundary layer cloud-drizzle processes, *JGR: Atmos.*, *122*, 4463-4478 <https://doi.org/10.1002/2016JD026326>, 2017.
- Wyant, M. C., Bretherton, C. S., Bacmeister, J. T., Kiehl, J. T., Held, I. M., Zhao, M., . . . Soden, B. J. J. C. D.: A comparison of low-latitude cloud properties and their response to climate change in three AGCMs sorted into regimes using mid-tropospheric vertical velocity, *Clim. Dyn.*, *27*, 261-279, <http://doi.org/10.1007/s00382-006-0138-4>, 2006.
- Yuan, L. J. J. n. A.: Increase of cloud droplet size with aerosol optical depth: An observation and modeling study, *JGR: Atmos.*, *113*, D4, <https://doi.org/10.1029/2007JD008632>, 2008.



Zeb, B., Alam, K., Sorooshian, A., Chishtie, F., Ahmad, I., Bibi, H. J. J. o. a., & physics, s.-t.: Temporal characteristics of aerosol optical properties over the glacier region of northern Pakistan, *Jour. Atmos. Sol-Terr. Phy.*, *186*, 35-46, <https://doi.org/10.1016/j.jastp.2019.02.004>, 2019.

Zhou, S., Yang, J., Wang, W.-C., Zhao, C., Gong, D., Shi, P. J. A. C., & Physics.: An observational study of the effects of aerosols on diurnal variation of heavy rainfall and associated clouds over Beijing–Tianjin–Hebei, *Atmos. Chem. Phy.*, *20*, 5211-5229, <https://doi.org/10.5194/acp-20-5211-2020>, 2020.